Title

Protracted and asynchronous accumulation of PSD95-family MAGUKs during maturation of nascent dendritic spines

Journal

Developmental Neurobiology, 77(10)

ISSN

1932-8451

Authors

Lambert, Jason T
Hill, Travis C
Park, Deborah K
et al.

Publication Date

2017-10-01

DOI

10.1002/dneu.22503

Peer reviewed

HHS Public Access

Author manuscript

Dev Neurobiol. Author manuscript; available in PMC 2018 October 01.

Published in final edited form as:

Dev Neurobiol. 2017 October ; 77(10): 1161–1174. doi:10.1002/dneu.22503.

Protracted and Asynchronous Accumulation of PSD95-family MAGUKs during Maturation of Nascent Dendritic Spines

Jason T. Lambert[1], **Travis C. Hill**[1], **Deborah K. Park**[1], **Julie H. Culp**[1], and **Karen Zito**[1,*]

[1]Center for Neuroscience, University of California Davis, Davis, California, 95618

Abstract

The formation and stabilization of new dendritic spines is a key component of the experience-dependent neural circuit plasticity that supports learning, but the molecular maturation of nascent spines remains largely unexplored. The PSD95-family of membrane-associated guanylate kinases (PSD-MAGUKs), most notably PSD95, has a demonstrated role in promoting spine stability. However, nascent spines contain low levels of PSD95, suggesting that other members of the PSD-MAGUK family might act to stabilize nascent spines in the early stages of spiny synapse formation. Here, we used GFP-fusion constructs to quantitatively define the molecular composition of new spines, focusing on the PSD-MAGUK family. We found that PSD95 levels in new spines were as low as those previously associated with rapid subsequent spine elimination, and new spines did not achieve mature levels of PSD95 until between 12 and 20 h following new spine identification. Surprisingly, we found that the PSD-MAGUKs PSD93, SAP97, and SAP102 were also substantially less enriched in new spines. However, they accumulated in new spines more quickly than PSD95: SAP102 enriched to mature levels within 3 h, SAP97 and PSD93 enriched gradually over the course of 6 h. Intriguingly, when we restricted our analysis to only those new spines that persisted, SAP97 was the only PSD-MAGUK already present at mature levels in persistent new spines when first identified. Our findings uncover a key structural difference between nascent and mature spines, and suggest a mechanism for the stabilization of nascent spines through the sequential arrival of PSD-MAGUKs.

Keywords

dendritic spine; PSD-MAGUK; structural plasticity; hippocampus; 2-photon imaging

INTRODUCTION

In the cerebral cortex, the structural plasticity of dendritic spines serves as a vital component of the experience-dependent circuit modifications that underlie learning. In particular, the

*Correspondence should be addressed to Karen Zito, Center for Neuroscience, University of California Davis, Davis, CA, 95618 USA. Tel: 530-752-7832; kzito@ucdavis.edu.

Author Contributions

J.T.L., T.C.H., and K.Z. designed experiments. Data were collected by J.T.L., T.C.H., and D.K.P., and analyzed by J.T.L, T.C.H., D.K.P., and J.H.C. The manuscript was written by J.T.L. and K.Z. All authors provided comments on the manuscript.

Competing Financial Interests Statement

The authors declare no competing financial interests.

formation and stabilization of new dendritic spines is a key initial step in the establishment of new connections between excitatory neurons. Indeed, *in vivo* imaging studies have shown that new spine outgrowth and stabilization are associated with learning (Xu et al., 2009; Yang et al., 2009; Roberts et al., 2010; Moczulska et al., 2013). Furthermore, new spine growth and stabilization have also been associated with long-term potentiation (LTP), a cellular mechanism thought to support learning and memory (Engert and Bonhoeffer, 1999; Maletic-Savatic et al., 1999; De Roo et al., 2008; Kwon and Sabatini, 2011; Hill and Zito, 2013), and with depolarizing GABAergic signaling (Oh et al., 2016). Notably, recent findings demonstrated that destabilization of those new spines whose growth is associated with learning a behavioral task resulted in loss of the learned behavior (Hayashi-Takagi et al., 2015), supporting that new spine growth and stabilization are essential for learning. However, the molecular mechanisms that drive the growth and stabilization of new spines remain poorly defined.

Members of the PSD95-family of MAGUK synaptic scaffolding proteins (PSD-MAGUKs), prominent components of the postsynaptic density (PSD), represent attractive candidates for molecules that could regulate nascent spine stabilization through their recruitment or modification by second messengers. PSD-MAGUKs have a stereotypical domain structure, consisting of three PDZ domains, a Src homology 3 (SH3) domain, and a nonfunctional guanylate kinase (GK) domain (Zheng et al., 2011). Via their PDZ domains, PSD-MAGUKs function to anchor at the synapse both α-amino-3-hydroxy-5-methyl-4-isoxazolepropionic acid receptors (AMPARs) and N-methyl-D-aspartate receptors (NMDARs), the principal glutamate receptors involved in synaptic transmission (Kim and Sheng, 2004). They also bind to guanylate kinase associated protein (GKAP) via their GK domains, which links them to the actin cytoskeleton (Zheng et al., 2011). PSD-MAGUKs thus serve as critical links between excitatory synaptic activity and the cytoskeletal proteins that determine the size and shape of the spine. Furthermore, the presence of PSD-MAGUK proteins, most notably PSD95, has been associated with increased synapse density and stability, while their absence has the opposite effect (El-Husseini et al., 2000; Okabe et al., 2001; Prange and Murphy, 2001; Nakagawa et al., 2004; Parker et al., 2004; Ehrlich et al., 2007; Woods et al., 2011; Cane et al., 2014). Intriguingly, it has been reported that new spines lacked puncta of PSD95 (De Roo et al., 2008), which should compromise their stability. We hypothesized that a different PSD-MAGUK acts to compensate for the absence of PSD95 and plays a greater role in new spines.

To test the relative roles of PSD-MAGUKs at nascent spines we used dual color two-photon time-lapse imaging to assess which GFP-tagged PSD-MAGUKs are present in new spines at first appearance and as the spine matured. As expected, we found that new spines had lower PSD95-GFP levels than their mature neighbors. In fact, PSD95-GFP enrichment in new spines was as low as that observed in mature spines destined for elimination within 1 h (Woods et al., 2011), and did not increase until between 12 and 20 h after new spines were first identified, yet many new spines survived. Surprisingly, new spines were also less enriched for PSD93-GFP, SAP97-GFP, and SAP102-GFP. However, they accumulated these PSD-MAGUKs to levels comparable to mature spines at different rates, but all within 6 h, suggesting independent mechanisms for their incorporation and/or retention in the new spine macromolecular complex. Our results reveal a striking difference in PSD-MAGUK content

between new and mature spines, and suggest a mechanism for the stabilization of nascent spines through the sequential arrival of PSD-MAGUKs.

METHODS

Preparation and transfection of organotypic slice cultures

Organotypic hippocampal slice cultures were prepared from P6–7 rats of both sexes, as described (Stoppini et al., 1991) in accordance with animal care and use guidelines of the University of California. Genes were delivered 1–2 days prior to imaging using particle-mediated gene transfer, as described (Woods and Zito, 2008), except 3–4 μg of GFP-tagged construct and/or 10–15 μg of DsRed-Express (Clontech) were coated onto 5.5–8 mg of 1.6 μm gold beads. GFP-tagged constructs included: 4 μg PSD93α-GFP (Schnell et al., 2002), 3–4 μg PSD95α-GFP (Gray et al., 2006), 4 μg SAP97β-GFP (Schnell et al., 2002), 3–4 μg SAP102-GFP (Schnell et al., 2002), and 3 μg Nrb1-GFP (Nakanishi et al., 1997).

Two-photon imaging

Image stacks (512 X 512 pixels, 1 μm z-steps) of 2–6 secondary and tertiary, apical and basal dendritic segments from hippocampal pyramidal neurons (7–12 DIV) were acquired on a custom two-photon laser scanning microscope with a pulsed Ti::Sapphire laser (930 nm, 0.5–3 mW at the sample; Spectra Physics, Newport). Data acquisition was controlled by ScanImage (Pologruto et al., 2003) written in MATLAB (MathWorks). All images shown are maximum projections of 3D image stacks after applying a median filter (3 X 3) to the raw image data. For time-lapse experiments lasting >3 h, images were acquired in slice culture medium at room temperature (RT) and the slice was maintained in the incubator (35°C) between acquisitions.

Definition of a new spine and estimation of spine size

New spines were defined as any protrusion emanating from the dendrite that was absent in the first image and present in the second image (90 min later) of the time-lapse series. Persistent, mature spines were defined as spines that were present in all images in the time-lapse series. If there was uncertainty concerning the status of a spine because of undulations in the dendrite, swellings in the z-axis, or spine movement, the spine was excluded. Spine size was estimated from bleed-through-corrected and background-subtracted red (DsRed-Express) fluorescence intensities by normalizing the integrated spine intensity value to the average red pixel intensity of the dendrite. Such spine brightness measurements give an accurate estimate of relative spine size when compared with electron microscopy (Holtmaat et al., 2005).

Quantification of relative enrichment of GFP-tagged proteins

Relative enrichment of GFP-tagged proteins in dendritic spines was calculated using bleed-through-corrected and background-subtracted green (GFP) and red (DsRed-Express) fluorescence intensities from spines and dendrites, similar to Woods *et al.* (2011). Briefly, the ratio of green fluorescence intensity to red fluorescence intensity (G/R) was calculated for each new spine, neighboring persistent spines (4–14), and three representative regions on the dendritic shaft (excluding regions containing prominent dendritic GFP puncta). To

quantify spine fluorescence intensities, boxes were drawn around whole spines and spine necks using custom software written in MATLAB. To remove fluorescent signal not originating from the spine, the integrated intensity of an identical box taken from a nearby spine-free segment of dendrite was subtracted. To compare each spine to the neighboring persistent spines on the same dendritic segment, relative enrichment for every spine was calculated by normalizing the G/R of the spine to the mean G/R of the persistent neighboring spines in the same image.

$$relative\ enrichment = \frac{(G/R)_{spine\ of\ interest} / \overline{(G/R)}_{dendrite}}{\overline{(G/R)}_{neighboring\ spines} / \overline{(G/R)}_{dendrite}} = \frac{(G/R)_{spine\ of\ interest}}{\overline{(G/R)}_{neighboring\ spines}}$$

We implemented several quality control measures. First, we excluded transfected cells that failed to express the GFP-tagged constructs at levels sufficient for accurate quantification, using standardized criteria: if, after background and bleedthrough subtraction, (1) the mean green pixel intensity (G) from persistent spines was less than a minimum value (3.23 a.u.), (2) the mean persistent spine G/R was less than a minimum value (0.01), or (3) the ratio of the square of the mean persistent spine G/R to the absolute value of the mean dendrite G/R was less than a minimum value (0.05). These criteria were selected because they consistently excluded cells that yielded negative pixel intensity values after background and bleedthrough subtraction. Second, all cells were excluded that exhibited significant photobleaching (a significant decrease in the average integrated green fluorescence intensity of persistent spines as compared to the first time point).

Statistics

Data are presented as mean ± SEM, statistics were calculated across cells, and significance was set at $p < 0.05$ (single-factor ANOVA with Fisher's LSD post-hoc test, unless otherwise noted). Single and double asterisks indicate $p < 0.05$ and $p < 0.001$, respectively.

RESULTS

New spines have lower PSD95-GFP levels than mature spines

To assess the relative levels of PSD-MAGUKs in new spines, we monitored GFP-tagged PSD-MAGUK levels (GFP) and spine morphology (DsRed-Express) using dual-color time-lapse two-photon imaging. We began our studies with PSD95, which was previously reported to be absent as puncta from new spines until 5–19 h after their initial appearance (De Roo et al., 2008). We set out to assess more quantitatively the content and accumulation of PSD95-GFP in new spines. Images of secondary and tertiary dendrites on hippocampal pyramidal neurons co-expressing DsRed-Express and PSD95-GFP were acquired at time intervals of 90 min. To account for variations in spine size, we quantified 'enrichment' of PSD95-GFP in new spines by normalizing the integrated fluorescence intensity in the spine head from PSD95-GFP (green, G) with that from the freely diffusible DsRed-Express (red, R), and this value was divided by the G/R ratio in the dendrite to normalize for expression levels. 'Relative enrichment' of PSD95-GFP in new spines was calculated by normalizing

the individual new spine enrichment with the average enrichment of the mature, persistent spines on the same dendritic segment (Fig. 1A).

We found that new spines (< 90 min old) had considerably lower enrichment levels of PSD95-GFP relative to that of neighboring spines (0.61 ± 0.04, $p < 0.001$; Fig. 1B, C). Because new spines were considerably smaller than their neighbors ($p < 0.001$; Fig. 1D), we also assessed whether spine size differences contributed to the observed differences in PSD95-GFP enrichment in new spines. To do this, we separated neighboring spines into two groups: 'small neighbors' were smaller than or within 1 standard deviation of the mean new spine size, 'large neighbors' were all others. Notably, new spines were considerably less enriched for PSD95-GFP when compared to small neighbors ($p < 0.001$; Fig. 1C), despite there being no significant difference between their sizes ($p = 0.57$; Fig. 1D). Furthermore, relative PSD95-GFP enrichment was not significantly different between small and large neighbors (1.02 ± 0.02 for small neighbors, 0.99 ± 0.02 for large neighbors, $p = 0.40$, Fig. 1C), again supporting that maturity and not spine size determined enrichment measurements. As new spines often are longer and thinner than mature spines, we performed a similar analysis using length to width ratio (L:W) and found again that, although new spines have higher L:W ratios, they were still significantly less enriched for PSD95-GFP than neighbors with similar L:W ratios ($p < 0.001$; Supplemental Figure 1). We conclude that new spines contain considerably lower levels of PSD95-GFP than their mature neighbors, independent of spine size or shape.

We observed that the vast majority of new spines (86%) contained PSD95-GFP levels below 1 standard deviation lower than the mean relative enrichment for neighboring spines (Fig. 1E). Considering that spines exhibiting such low levels of PSD95-GFP are predominantly those destined for elimination within 1 h (Woods et al., 2011), we expected that those new spines that stabilized and persisted throughout the time-lapse imaging session would accumulate enhanced levels of PSD95-GFP within an hour of outgrowth. To address whether PSD95-GFP enriched in new spines within hours after outgrowth, we performed extended time-lapse experiments in which dendritic segments were imaged at intervals of 90 min for 7.5 h (Fig. 2A). In contrast to our expectation, the relative PSD95-GFP enrichment of new spines remained significantly less than that of neighboring spines ($p < 0.05$ for all time-points, heteroscedastic *t*-test; Fig. 2B, blue), and new spines did not display any significant increase in relative PSD95-GFP enrichment over the entire imaging session ($p = 0.95$, paired *t*-test; Fig. 2C). To determine when new spines achieve mature PSD95-GFP levels, we performed additional time-lapse experiments using longer imaging intervals. Even12 h after identification, enrichment of PSD95-GFP still had not increased in new spines (0.79 ± 0.08) beyond enrichment levels observed at t = 0 (0.70 ± 0.05; $p = 0.13$; Fig. 2D, E); however, by 20 h after identification, PSD95-GFP enrichment had finally reached levels in new spines (1.12 ± 0.10) indistinguishable from that of mature neighbors (1.00 ± 0.00; $p = 0.35$; Fig. 2D, E). Thus, we conclude that PSD95-GFP levels do not increase in new spines within 12 h after outgrowth, instead persisting at the low levels that are observed in spines that are eliminating (Woods et al., 2011) until finally reaching mature levels between 12 and 20 h. We therefore hypothesized that another PSD-MAGUK compensates for the low levels of PSD95, acting to stabilize nascent spines in the early stages of spine development.

New spines have even lower levels of PSD93-GFP, but accumulate mature levels within 4.5 h

Because PSD93 is closely related to PSD95 (Brenman et al., 1996; Kim et al., 1996), and may be the principle MAGUK at a subset of hippocampal synapses (Elias et al., 2006), we reasoned that PSD93 might play the primary role in stabilizing new spines. We therefore measured the PSD93-GFP content as new spines matured on dendrites of hippocampal pyramidal neurons co-transfected with PSD93-GFP and DsRed-Express. Surprisingly, we found that the enrichment for PSD93-GFP in new spines relative to neighboring spines (0.29 ± 0.05, $p < 0.001$; Fig. 3A, B) was even lower than that of PSD95-GFP. This lower enrichment in new spines was independent of spine size or shape, as new spines were less enriched for PSD93-GFP than sized-matched ($p < 0.001$; Fig. 3B, C) or shape-matched ($p < 0.001$; Supplemental Figure 1) neighboring spines. Notably, extended time-lapse experiments revealed a key difference between PSD95-GFP and PSD93-GFP: although new spines failed to enrich for PSD95-GFP over 12 h, enrichment for PSD93-GFP gradually increased in new spines, until reaching mature levels within 4.5 h after the new spines were identified (0.82 ± 0.11 at t = 270 min; $p = 0.12$, heteroscedastic *t*-test; Fig. 3D). We conclude that PSD93, while even less enriched than PSD95 at the earliest stages of new spine development, could serve a key role in stabilizing new spines within the first few hours of new spine outgrowth.

New spines have low levels of SAP97-GFP and SAP102-GFP, but accumulate mature levels of SAP102-GFP within 90 min and SAP97-GFP within 4.5 h

The low levels of both PSD93-GFP and PSD95-GFP at the earliest stages of new spine development suggested that there could be an additional PSD-MAGUK with a greater role at these earliest time points. Because the PSD-MAGUKs SAP102 and SAP97 also have demonstrated roles in regulating synapse stability (Nakagawa et al., 2004; Elias et al., 2006; Chen et al., 2011; Levy et al., 2015), and SAP102 has previously been implicated in early synapse development (Sans et al., 2000; Elias et al., 2008; Murata and Constantine-Paton, 2013), we examined whether SAP102 or SAP97 might arrive early to stabilize nascent spines. We therefore measured the content of GFP-tagged SAP97 or SAP102 as new spines matured on dendrites of hippocampal pyramidal neurons co-transfected with either SAP97-GFP or SAP102-GFP and DsRed-Express. Similar to PSD93-GFP and PSD95-GFP, we found that SAP97-GFP and SAP102-GFP were less enriched in new spines compared to neighboring spines (0.70 ± 0.05 for SAP97-GFP, $p < 0.001$, and 0.63 ± 0.04 for SAP102-GFP, $p < 0.001$; Fig. 4A,B), even when controlling for spine size ($p < 0.001$ for both SAP97-GFP and SAP102-GFP; Fig. 4B, C) and shape ($p < 0.001$ for both SAP97-GFP and SAP102-GFP; Supplemental Figure 1). Like PSD93-GFP, our extended time-lapse experiments showed that SAP97-GFP reached mature levels 4.5 h after new spines were first identified (0.91 ± 0.10 at t = 270 min, $p = 0.40$, heteroscedastic *t*-test; Fig. 4D). However, in contrast to the gradual enrichment observed for PSD93-GFP and SAP97-GFP, SAP102-GFP reached mature levels within 90 min of new spine identification (0.87 ± 0.07, $p = 0.10$, heteroscedastic *t*-test; Fig. 4D), suggesting that SAP102 indeed could be a major player at these earliest time points.

SAP97-GFP is at mature levels in persistent new spines when they first appear

Intriguingly, when we separately examined new spines that persisted for the entire 6 h of the time-lapse experiment, we found that persistent new spines were already as enriched for SAP97-GFP as their neighbors at first appearance (0.85 ± 0.11, p = 0.20; Fig. 5A, B). In contrast, transient new spines lasting <90 min were less enriched for SAP97-GFP (0.67 ± 0.10, p < 0.01; Fig. 5A, B) than were neighboring spines. There was no difference, however, between the initial relative enrichment levels in transient versus persistent new spines for any of the other PSD-MAGUKs: SAP102-GFP (0.69 ± 0.09 transient, 0.73 ± 0.10 persistent, p = 0.73; Fig. 5C), PSD93-GFP (0.31 ± 0.08 transient, 0.36 ± 0.09 persistent, p = 0.61; Fig. 5D) or PSD95-GFP (0.55 ± 0.04 transient, 0.65 ± 0.09 persistent, p = 0.12; Fig. 5E). Although new spines that persisted trended toward being larger (104.2 ± 11.0) than the transient new spines (73.1 ± 10.3; p = 0.19), both groups were considerably smaller than mature neighbors (229.7 ± 20.8; p < 0.001 for both; Supplemental Figure 2A). In addition, there was no correlation between a spine's estimated size and relative enrichment for SAP97-GFP (new spines: r = −0.10, p = 0.36; neighboring spines: r = −0.02, p = 0.71; Pearson's correlation; Supplemental Figure 2B, C), supporting that SAP97-GFP enrichment associated with persistent new spines is not simply due to increased size. We therefore conclude that the initial levels of SAP97 may be a determining factor in new spine stabilization.

Arrival times of the PSD-MAGUKs at new spines are not correlated with expression levels

One potential caveat of our experiments is that PSD-MAGUK levels in new spines could be influenced by levels of overexpression of the GFP-tagged proteins; perhaps those proteins expressed at higher levels appear in new spines earlier. For this study, we endeavored to overexpress GFP-tagged PSD-MAGUKs at the lowest levels possible for accurate measurement, which was also important because strong overexpression of PSD-MAGUKs, such as PSD95, has been shown to increase both spine size and spine density (El-Husseini et al., 2000). In our experiments, we expressed PSD-MAGUKs at low enough levels that new spine size and spine density were not different compared to control cells expressing only DsRed-Express (Fig. 6A, B). To determine whether higher expression levels corresponded to earlier arrival times in new spines, we estimated GFP-MAGUK expression level from the green fluorescence intensity in persistent spines, normalized to the dendritic red fluorescence intensity to control for image brightness (Fig. 6C). Notably, this overexpression estimate did not correspond to the sequence of PSD-MAGUK arrival. Indeed, overexpression was highest for cells expressing PSD95-GFP (0.11 ± 0.03 a.u.), yet PSD95-GFP did not accumulate in new spines for over 12 h. Conversely, SAP102-GFP was intermediately overexpressed (0.06 ± 0.01 a.u.) but was the earliest PSD-MAGUK to arrive at new spines. Furthermore, expression level was not correlated with the magnitude of change in relative enrichment of PSD-MAGUKs in new spines over the course of the time-lapse experiment (r = −0.57, p = 0.43, Pearson's correlation; Fig. 6D). Thus, we conclude that individual PSD-MAGUKs arrive at new spines at different times, independent of expression level, likely supported by selective targeting and/or anchoring mechanisms.

The actin-binding protein, Neurabin I, is at mature levels in new spines

Because new spines less than 90 min old were on average less enriched for every GFP-tagged PSD-MAGUK we had investigated, we wondered whether lowered protein enrichment was a general property of new spines. Previous studies have shown that the first proteins to appear in mature spines following a robust stimulus resulting in structural growth are proteins that bind and regulate the actin cytoskeleton (Bosch et al., 2014). We therefore decided to examine the arrival time of the actin-binding protein, Neurabin I (Nakanishi et al., 1997), which has been shown to be highly localized to dendritic spines (Zito et al., 2004). As expected, we found that Nrb1-GFP rapidly arrived in new spines (Fig. 7A). Indeed, new spines were as enriched for Nrb1-GFP as neighboring spines, independent of spine size (0.94 ± 0.07, $p = 0.69$; Fig. 7B, C). Thus, the asynchronous and delayed arrival of PSD-MAGUKs in nascent spines does not appear to be due to a difficulty of protein delivery or retention in new spines, but instead likely signifies a tightly regulated process, which could represent a mechanism for the stabilization of nascent spines through the sequential arrival of PSD-MAGUKs.

DISCUSSION

In this study, we defined the relative roles of specific PSD-MAGUK family members in the development of nascent dendritic spines by quantitatively examining their arrival times. Given reports that new spines were devoid of PSD95 puncta for more than 5 hours after initial outgrowth (De Roo et al., 2008), despite the critical role of PSD95 in supporting spine stability (Ehrlich et al., 2007; Woods et al., 2011; Cane et al., 2014), we hypothesized that additional PSD-MAGUK family members would accumulate in new spines to support their growth and stabilization in these earliest stages of spine development. In fact, there is considerable functional overlap between the different PSD-MAGUKs. PSD93 and PSD95, for example, play similar roles supporting basal synaptic transmission in the hippocampus, but in largely non-overlapping populations of synapses (Elias et al., 2006). Additionally, expression of SAP102 is upregulated in the absence of PSD93 and PSD95, indicating a possible compensatory mechanism (Elias et al., 2006). Indeed, SAP102 is the primary MAGUK at excitatory synapses during early development rather than PSD95 (Sans et al., 2000; Elias et al., 2008). For these reasons, we were surprised to find that none of the PSD-MAGUK family members we examined showed increased expression levels to compensate for reduced expression levels of PSD95; instead, all were initially at considerably lower levels in new spines as compared to their persistent neighbors (summarized in Fig. 8A).

We demonstrated that individual PSD-MAGUKs reached mature levels in nascent spines at different times (summarized in Fig. 8B): SAP102 arrived first, followed by SAP97 and PSD93. PSD95 arrives last with a delay of up to 20 h. This parallels the progression of development, when SAP102 provides the MAGUK scaffolding role at newly developing synapses early in development, and is later largely replaced by PSD93 and PSD95 (Sans et al., 2000; Elias et al., 2008). However, when we segregated new spines based on stability for the entire 6 hours of our time-lapse experiments, we discovered a population of persistent new spines already enriched for SAP97-GFP at their first appearance, indicating that new spines destined to persist more than 6 hours rapidly accumulated SAP97-GFP, even before

enriching for SAP102-GFP. Since phosphorylation of SAP97 by CaMKII drives SAP97 accumulation in spines (Mauceri et al., 2004), perhaps this rapid accumulation of SAP97 in persistent new spines indicates a higher level of synaptic activity at these spines (Hill and Zito, 2013) that leads to SAP97 recruitment and their stabilization. Conversely, the lack of a difference in initial enrichment for SAP102-GFP, PSD93-GFP, and PSD95-GFP between transient and persistent new spines might suggest an activity-independent, gradual recruitment of these PSD-MAGUKs.

Why do spines accumulate different PSD-MAGUKs at different time-points during their maturation? Perhaps each type of PSD-MAGUK imparts a new level of stability to the maturing spine. SAP102, for example, could enrich the 1.5–3 h old spine with GluN2B containing NMDARs. This variant of the NMDAR binds to activated CaMKII and recruits it to the synapse, placing CaMKII in close proximity to both Ca^{2+} (entering the spine through the NMDAR) and substrates for phosphorylation, such as AMPARs (Barria and Malinow, 2005; Zhou et al., 2007). A new spine with a PSD composed primarily of SAP102, might therefore be poised for plasticity. Later, the arrival of PSD93 and GluN2A-containing NMDARs could stabilize the response of the spine to glutamatergic inputs, perhaps slowing spine enlargement and LTP, but also making spine shrinkage and elimination less likely. The PDZ domains of PSD93 are remarkably similar to the PDZ domains of PSD95 in sequence and structure (Fiorentini et al., 2009). The 4.5–6 h old spine, containing mature levels of SAP102, SAP97, and PSD93, yet still substantially less enriched for PSD95, might recruit a complement of proteins similar to a mature PSD, but retain the flexibility to undergo further plasticity. The late arrival of PSD95 might therefore be reserved for those synapses that must be stabilized only when incorporated into circuits vital for the function or survival of the animal.

The stratification of arrival times that we observed for the different PSD-MAGUKs suggests that they are recruited to new spines through independent mechanisms. For example, differential requirements for palmitoylation for synaptic targeting could independently regulate arrival times. Since PSD95 requires palmitoylation at its N-terminus in order to be recruited to spines (El-Husseini et al., 2000; El-Husseini et al., 2002; Ehrlich and Malinow, 2004), downregulation of palmitoylating enzymes or the upregulation of depalmitoylating enzymes could exclude PSD95 from new spines. In contrast, although it is N-terminally palmitoylated similar to PSD95, PSD93 does not require palmitoylation for synaptic localization (Firestein et al., 2000). Synaptic localization of PSD93 and SAP102 is N-terminally dependent by an unknown mechanism. Chimeric proteins which graft the N-terminus of PSD93 or SAP102 to the palmitoylation-deficient mutant PSD95 successfully localize to synapses, even when the palmitoylated cysteines of PSD93 are mutated (Firestein et al., 2000). The differences in arrival times between PSD93, SAP102, and SAP97 may be due to differences in binding affinities for synaptic proteins. Although PSD-MAGUKs bind to many of the same binding partners, differences in substrate affinity have been described using small molecule inhibitors (Nissen et al., 2015). A-kinase Anchoring Protein (AKAP) 79/150 is one PSD-MAGUK binding partner that has been shown to regulate spine size and density, and may recruit PSD-MAGUKs to spines (Robertson et al., 2009), making AKAP79/150 an attractive candidate for a protein that controls the selective recruitment of PSD-MAGUKs to new spines.

What is the functional consequence of protracted MAGUK arrival times? Notably, new spines have AMPAR-mediated EPSCs with amplitudes similar to pre-existing spines (Zito et al., 2009; Kwon and Sabatini, 2011). As PSD-MAGUKs have critically important roles for maintaining AMPARs and NMDARs at pre-existing spines (Elias et al., 2006; Schlüter et al., 2006; Chen et al., 2015; Levy et al., 2015), it is not clear what serves as the scaffold that supports basal synaptic transmission at nascent spines. We found that new spines that persisted for >6 h initially had levels of SAP97-GFP that were comparable to neighboring persistent spines. Since SAP97 binds GluA1 (Leonard et al., 1998) and has been shown to deliver AMPARs to synapses in response to activity (Rumbaugh et al., 2003; Schlüter et al., 2006; Zheng and Keifer, 2014), SAP97 could deliver AMPARs to a subset of new spines undergoing LTP. However, recent studies of SAP97 KO mice have indicated that SAP97 does not play a role in basal AMPAR recruitment to synapses (Howard et al., 2010), and cannot compensate for triple-KD of the other PSD-MAGUKs (Levy et al., 2015). SAP97 acting alone is therefore unlikely to explain how the baseline AMPAR EPSCs of new spines resemble those of mature spines. Other AMPAR-clustering scaffolding proteins likely play a greater role at new spines. Potential candidates include MAGI-2, a member of the Membrane Associated Guanylate kinases with Inverted orientation (MAGIs), a protein family that shares evolutionary history with the PSD-MAGUKs (Danielson et al., 2012), and the actin-spectrin-binding protein 4.1N, which binds directly to both actin and the AMPAR subunit GluA1 (Shen et al., 2000) and recruits SAP97 to synapses (Lue et al., 1994; Rumbaugh et al., 2003). Future studies will determine the identity of the proteins that regulate clustering of AMPARs to support early synaptic transmission at nascent spiny synapses.

Supplementary Material

Refer to Web version on PubMed Central for supplementary material.

Acknowledgments

This work was supported by the National Science Foundation (0845285), an NIH Training Grant (T32GM007377) and a NARSAD Independent Investigator Grant from the Brain & Behavior Research Foundation (23312). We thank J. Jahncke for technical support; I. Stein, M. Burns, H.J. Cheng, E. Diaz, and L. Tian for valuable discussion; L. Parajuli, O. Vivas, J. Jahncke, L. Kirk and K. Plambeck for critical reading of the manuscript.

References

Barria A, Malinow R. NMDA receptor subunit composition controls synaptic plasticity by regulating binding to CaMKII. Neuron. 2005; 48:289–301. [PubMed: 16242409]

Bosch M, Castro J, Saneyoshi T, Matsuno H, Sur M, Hayashi Y. Structural and molecular remodeling of dendritic spine structures during long-term potentiation. Neuron. 2014; 82:444–459. [PubMed: 24742465]

Brenman JE, Christopherson KS, Craven SE, McGee AW, Bredt DS. Cloning and characterization of postsynaptic density 93, a nitric oxide synthase interacting protein. J Neurosci. 1996; 16:7407–7415. [PubMed: 8922396]

Cane M, Maco B, Knott G, Holtmaat A. The relationship between PSD-95 clustering and spine stability in vivo. J Neurosci. 2014; 34:2075–2086. [PubMed: 24501349]

Chen BS, Thomas EV, Sanz-Clemente A, Roche KW. NMDA receptor-dependent regulation of dendritic spine morphology by SAP102 splice variants. J Neurosci. 2011; 31:89–96. [PubMed: 21209193]

Chen X, Levy JM, Hou A, Winters C, Azzam R, Sousa AA, Leapman RD, Nicoll RA, Reese TS. PSD-95 family MAGUKs are essential for anchoring AMPA and NMDA receptor complexes at the postsynaptic density. Proc Natl Acad Sci U S A. 2015; 112:E6983–6992. [PubMed: 26604311]

Danielson E, Zhang N, Metallo J, Kaleka K, Shin SM, Gerges N, Lee SH. S-SCAM/MAGI-2 is an essential synaptic scaffolding molecule for the GluA2-containing maintenance pool of AMPA receptors. J Neurosci. 2012; 32:6967–6980. [PubMed: 22593065]

De Roo M, Klauser P, Mendez P, Poglia L, Muller D. Activity-dependent PSD formation and stabilization of newly formed spines in hippocampal slice cultures. Cereb Cortex. 2008; 18:151–161. [PubMed: 17517683]

Ehrlich I, Klein M, Rumpel S, Malinow R. PSD-95 is required for activity-driven synapse stabilization. Proc Natl Acad Sci USA. 2007; 104:4176–4181. [PubMed: 17360496]

Ehrlich I, Malinow R. Postsynaptic density 95 controls AMPA receptor incorporation during long-term potentiation and experience-driven synaptic plasticity. J Neurosci. 2004; 24:916–927. [PubMed: 14749436]

El-Husseini AE-D, Schnell E, Dakoji S, Sweeney N, Zhou Q, Prange O, Gauthier-Campbell C, Aguilera-Moreno A, Nicoll RA, Bredt DS. Synaptic strength regulated by palmitate cycling on PSD-95. Cell. 2002; 108:849–863. [PubMed: 11955437]

El-Husseini AE, Craven SE, Chetkovich DM, Firestein BL, Schnell E, Aoki C, Bredt DS. Dual palmitoylation of PSD-95 mediates its vesiculotubular sorting, postsynaptic targeting, and ion channel clustering. J Cell Biol. 2000; 148:159–172. [PubMed: 10629226]

El-Husseini AE, Schnell E, Chetkovich DM, Nicoll RA, Bredt DS. PSD-95 involvement in maturation of excitatory synapses. Science. 2000; 290:1364–1368. [PubMed: 11082065]

Elias GM, Elias LA, Apostolides PF, Kriegstein AR, Nicoll RA. Differential trafficking of AMPA and NMDA receptors by SAP102 and PSD-95 underlies synapse development. Proc Natl Acad Sci U S A. 2008; 105:20953–20958. [PubMed: 19104036]

Elias GM, Funke L, Stein V, Grant SG, Bredt DS, Nicoll RA. Synapse-specific and developmentally regulated targeting of AMPA receptors by a family of MAGUK scaffolding proteins. Neuron. 2006; 52:320.

Engert F, Bonhoeffer T. Dendritic spine changes associated with hippocampal long-term synaptic plasticity. Nature. 1999; 399:66–70. [PubMed: 10331391]

Fiorentini M, Nielsen AK, Kristensen O, Kastrup JS, Gajhede M. Structure of the first PDZ domain of human PSD-93. Acta Crystallogr Sect F Struct Biol Cryst Commun. 2009; 65:1254–1257.

Firestein BL, Craven SE, Bredt DS. Postsynaptic targeting of MAGUKs mediated by distinct N-terminal domains. NeuroReport. 2000; 11:3479–3484. [PubMed: 11095503]

Gray NW, Weimer RM, Bureau I, Svoboda K. Rapid redistribution of synaptic PSD-95 in the neocortex in vivo. PLoS Biol. 2006; 4:e370. [PubMed: 17090216]

Hayashi-Takagi A, Yagishita S, Nakamura M, Shirai F, Wu YI, Loshbaugh AL, Kuhlman B, Hahn KM, Kasai H. Labelling and optical erasure of synaptic memory traces in the motor cortex. Nature. 2015; 525:333–338. [PubMed: 26352471]

Hill TC, Zito K. LTP-induced long-term stabilization of individual nascent dendritic spines. J Neurosci. 2013; 33:678–686. [PubMed: 23303946]

Holtmaat AJGD, Trachtenberg JT, Wilbrecht L, Shepherd GM, Zhang X, Knott GW, Svoboda K. Transient and persistent dendritic spines in the neocortex in vivo. Neuron. 2005; 45:279–291. [PubMed: 15664179]

Howard MA, Elias GM, Elias LAB, Swat W, Nicoll RA. The role of SAP97 in synaptic glutamate receptor dynamics. Proc Natl Acad Sci USA. 2010; 107:3805–3810. [PubMed: 20133708]

Kim E, Cho KO, Rothschild A, Sheng M. Heteromultimerization and NMDA receptor-clustering activity of Chapsyn-110, a member of the PSD-95 family of proteins. Neuron. 1996; 17:103–113. [PubMed: 8755482]

Kim E, Sheng M. PDZ domain proteins of synapses. Nat Rev Neurosci. 2004; 5:771–781. [PubMed: 15378037]

Kwon H-B, Sabatini BL. Glutamate induces de novo growth of functional spines in developing cortex. Nature. 2011; 474:100–104. [PubMed: 21552280]

Leonard AS, Davare MA, Horne MC, Garner CC, Hell JW. SAP97 is associated with the alpha-amino-3-hydroxy-5-methylisoxazole-4-propionic acid receptor GluR1 subunit. J Biol Chem. 1998; 273:19518–19524. [PubMed: 9677374]

Levy JM, Chen X, Reese TS, Nicoll RA. Synaptic Consolidation Normalizes AMPAR Quantal Size following MAGUK Loss. Neuron. 2015; 87:534–548. [PubMed: 26247861]

Lue RA, Marfatia SM, Branton D, Chishti AH. Cloning and characterization of hdlg: the human homologue of the Drosophila discs large tumor suppressor binds to protein 4.1. Proc Natl Acad Sci USA. 1994; 91:9822.

Maletic-Savatic M, Malinow R, Svoboda K. Rapid dendritic morphogenesis in CA1 hippocampal dendrites induced by synaptic activity. Science. 1999; 283:1923–1927. [PubMed: 10082466]

Mauceri D, Cattabeni F, Di Luca M, Gardoni F. Calcium/calmodulin-dependent protein kinase II phosphorylation drives synapse-associated protein 97 into spines. J Biol Chem. 2004; 279:23813–23821. [PubMed: 15044483]

Moczulska KE, Tinter-Thiede J, Peter M, Ushakova L, Wernle T, Bathellier B, Rumpel S. Dynamics of dendritic spines in the mouse auditory cortex during memory formation and memory recall. Proc Natl Acad Sci U S A. 2013; 110:18315–18320. [PubMed: 24151334]

Murata Y, Constantine-Paton M. Postsynaptic density scaffold SAP102 regulates cortical synapse development through EphB and PAK signaling pathway. J Neurosci. 2013; 33:5040–5052. [PubMed: 23486974]

Nakagawa T, Futai K, Lashuel HA, Lo I, Okamoto K, Walz T, Hayashi Y, Sheng M. Quaternary structure, protein dynamics, and synaptic function of SAP97 controlled by L27 domain interactions. Neuron. 2004; 44:453–467. [PubMed: 15504326]

Nakanishi H, Obaishi H, Satoh A, Wada M, Mandai K, Satoh K, Nishioka H, Matsuura Y, Mizoguchi A, Takai Y. Neurabin: A novel neural tissue-specific actin filament-binding protein involved in neurite formation. J Cell Biol. 1997; 139:951–961. [PubMed: 9362513]

Nissen KB, Haugaard-Kedstrom LM, Wilbek TS, Nielsen LS, Aberg E, Kristensen AS, Bach A, Jemth P, Stromgaard K. Targeting protein-protein interactions with trimeric ligands: high affinity inhibitors of the MAGUK protein family. PLoS One. 2015; 10:e0117668. [PubMed: 25658767]

Oh WC, Lutzu S, Castillo PE, Kwon HB. De novo synaptogenesis induced by GABA in the developing mouse cortex. Science. 2016; 353:1037–1040. [PubMed: 27516412]

Okabe S, Miwa A, Okado H. Spine formation and correlated assembly of presynaptic and postsynaptic molecules. J Neurosci. 2001; 21:6105–6114. [PubMed: 11487634]

Parker MJ, Zhao S, Bredt DS, Sanes JR, Feng G. PSD93 regulates synaptic stability at neuronal cholinergic synapses. J Neurosci. 2004; 24:378–388. [PubMed: 14724236]

Pologruto TA, Sabatini BL, Svoboda K. ScanImage: flexible software for operating laser scanning microscopes. Biomed Eng Online. 2003; 2:13. [PubMed: 12801419]

Prange O, Murphy TH. Modular transport of postsynaptic density-95 clusters and association with stable spine precursors during early development of cortical neurons. J Neurosci. 2001; 21:9325–9333. [PubMed: 11717366]

Roberts TF, Tschida KA, Klein ME, Mooney R. Rapid spine stabilization and synaptic enhancement at the onset of behavioural learning. Nature. 2010; 463:948–952. [PubMed: 20164928]

Robertson HR, Gibson ES, Benke TA, Dell'Acqua ML. Regulation of postsynaptic structure and function by an A-kinase anchoring protein-membrane-associated guanylate kinase scaffolding complex. J Neurosci. 2009; 29:7929–7943. [PubMed: 19535604]

Rumbaugh G, Sia G-M, Garner CC, Huganir RL. Synapse-associated protein-97 isoform-specific regulation of surface AMPA receptors and synaptic function in cultured neurons. J Neurosci. 2003; 23:4567–4576. [PubMed: 12805297]

Sans N, Petralia RS, Wang YX, Blahos J, Hell JW, Wenthold RJ. A developmental change in NMDA receptor-associated proteins at hippocampal synapses. J Neurosci. 2000; 20:1260–1271. [PubMed: 10648730]

Schlüter OM, Xu W, Malenka RC. Alternative N-terminal domains of PSD-95 and SAP97 govern activity-dependent regulation of synaptic AMPA receptor function. Neuron. 2006; 51:99–111. [PubMed: 16815335]

Schnell E, Sizemore M, Karimzadegan S, Chen L, Bredt DS, Nicoll RA. Direct interactions between PSD-95 and stargazin control synaptic AMPA receptor number. Proc Natl Acad Sci USA. 2002; 99:13902–13907. [PubMed: 12359873]

Shen L, Liang F, Walensky LD, Huganir RL. Regulation of AMPA receptor GluR1 subunit surface expression by a 4.1 N-linked actin cytoskeletal association. J Neurosci. 2000; 20:7932–7940. [PubMed: 11050113]

Stoppini L, Buchs PA, Muller D. A simple method for organotypic cultures of nervous tissue. J Neurosci Methods. 1991; 37:173–182. [PubMed: 1715499]

Woods G, Zito K. Preparation of gene gun bullets and biolistic transfection of neurons in slice culture. J Vis Exp. 2008 pii:e675.

Woods GF, Oh WC, Boudewyn LC, Mikula SK, Zito K. Loss of PSD-95 enrichment is not a prerequisite for spine retraction. J Neurosci. 2011; 31:12129–12138. [PubMed: 21865455]

Xu T, Yu X, Perlik AJ, Tobin WF, Zweig JA, Tennant K, Jones T, Zuo Y. Rapid formation and selective stabilization of synapses for enduring motor memories. Nature. 2009; 462:915–919. [PubMed: 19946267]

Yang G, Pan F, Gan WB. Stably maintained dendritic spines are associated with lifelong memories. Nature. 2009; 462:920–924. [PubMed: 19946265]

Zheng CY, Seabold GK, Horak M, Petralia RS. MAGUKs, synaptic development, and synaptic plasticity. The Neuroscientist. 2011; 17:493–512. [PubMed: 21498811]

Zheng Z, Keifer J. Sequential delivery of synaptic GluA1- and GluA4-containing AMPA receptors (AMPARs) by SAP97 anchored protein complexes in classical conditioning. J Biol Chem. 2014; 289:10540–10550. [PubMed: 24567325]

Zhou Y, Takahashi E, Li W, Halt A, Wiltgen B, Ehninger D, Li GD, Hell JW, Kennedy MB, Silva AJ. Interactions between the NR2B receptor and CaMKII modulate synaptic plasticity and spatial learning. J Neurosci. 2007; 27:13843–13853. [PubMed: 18077696]

Zito K, Knott G, Shepherd GMG, Shenolikar S, Svoboda K. Induction of spine growth and synapse formation by regulation of the spine actin cytoskeleton. Neuron. 2004; 44:321–334. [PubMed: 15473970]

Zito K, Scheuss V, Knott G, Hill T, Svoboda K. Rapid functional maturation of nascent dendritic spines. Neuron. 2009; 61:247–258. [PubMed: 19186167]

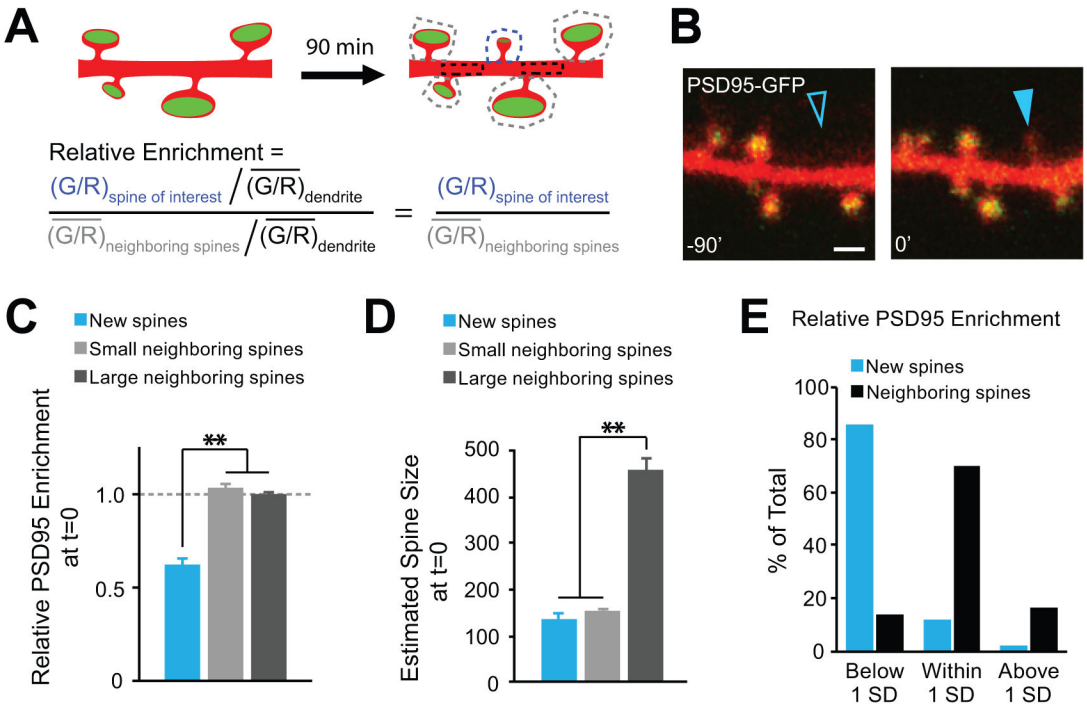

Figure 1. New spines have lower PSD95-GFP levels than mature spines

(A) Schematic representation of experiment and analysis. Relative enrichment reports the enrichment of a GFP-tagged protein in a spine of interest normalized to its average enrichment in neighboring spines. **(B)** Images of a dendrite on a hippocampal CA1 neuron (DIV 8) expressing PSD95-GFP and DsRed-Express. A site of new spine growth is marked with blue arrowheads before (open) and after (solid) initial appearance. Scale bar: 1 μm. **(C)** New spines are less enriched for PSD95-GFP than both small and large neighboring spines. **(D)** New spines were not smaller than small neighboring spines, but were considerably smaller than large neighboring spines. **(E)** Percentage of new (blue bars) or neighboring (black bars) spines that were lower than 1 SD less enriched for PSD95-GFP, within 1 SD, or greater than 1 SD more enriched for PSD95-GFP than the mean of the neighboring spines on the same dendrite. n = 92 new, 315 neighboring (153 small and 162 large) spines, 25 cells; *$p < 0.05$, **$p < 0.001$.

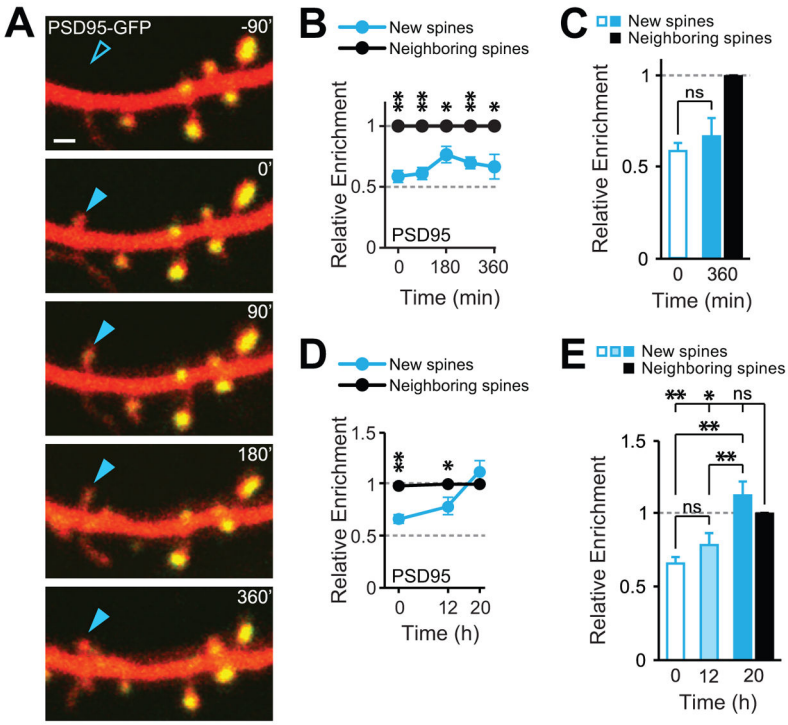

Figure 2. New spines do not accumulate mature levels of PSD95-GFP until 12–20 h

(A) Images of a dendrite on a CA1 neuron (DIV 10) expressing PSD95-GFP and DsRed-Express. Blue arrowheads mark a site of new spine growth before (open) and after (solid) initial appearance. Scale bar: 1 μm. **(B)** PSD95-GFP enrichment was lower in new spines (blue; 43 spines, 15 cells) compared to neighboring spines (black; 162 spines, 15 cells) at every time-point. **(C)** PSD95-GFP enrichment in new spines (blue) did not increase from baseline levels over the course of 6 h. **(D)** PSD95-GFP enrichment in new spines at 12 h (79 spines, 24 persisting to 12 h, 12 cells) remained lower than neighboring spines; however, at 20 h (47 spines, 5 persisting to 20 h, 6 cells), new spines reached mature levels of PSD95-GFP. **(E)** PSD95-GFP enrichment in new spines at 12 h was not different than baseline (0 h), but had increased to mature levels by 20 h. Significance for each time-point of **B** and **D** was determined using a heteroscedastic Student's *t*-test; significance for **C** was determined using a paired *t*-test; *p < 0.05, **p < 0.001.

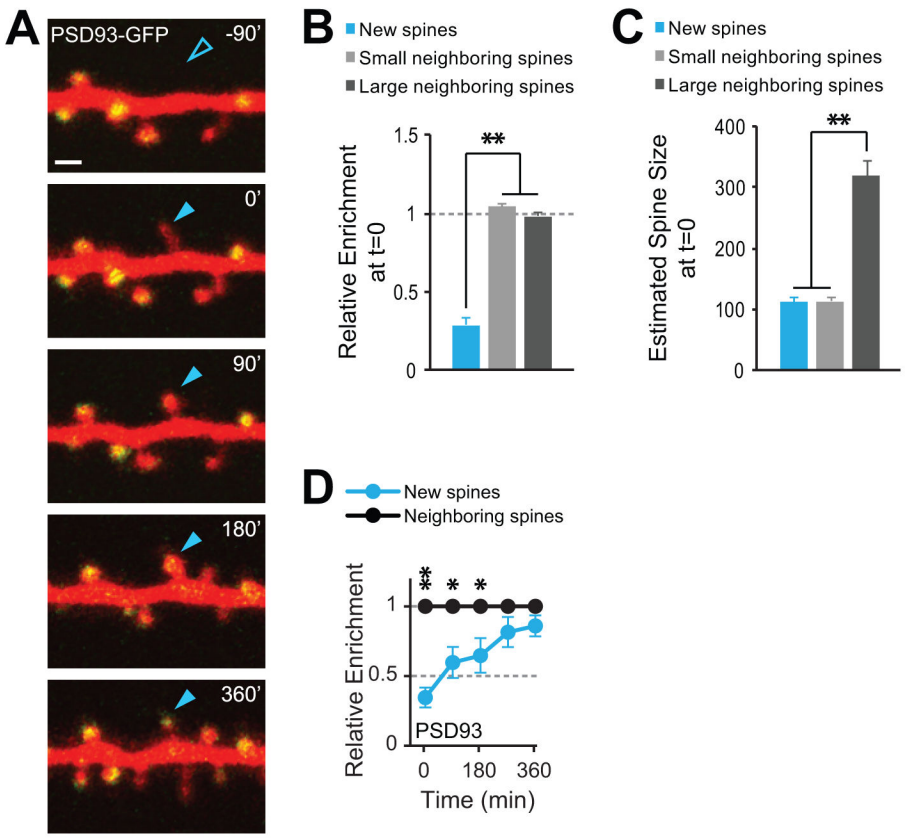

Figure 3. New spines have even lower levels of PSD93-GFP but accumulate mature levels within 4.5 h

(A) Images of a dendrite on a CA1 neuron (DIV 7) expressing PSD93-GFP and DsRed-Express. Blue arrowheads mark the site of new spine growth before (open) and after (solid) initial appearance. Scale bar: 1 μm. **(B)** New spines are less enriched for PSD93-GFP than both small and large neighboring spines. n = 121 new, 350 neighboring (180 small and 170 large) spines, 24 cells. **(C)** New spines were not smaller than small neighboring spines, but were considerably smaller than large neighboring spines. **(D)** Relative enrichment of new spines (blue; 61 spines, 14 cells) is plotted over time relative to neighboring persistent spines (black; 164 spines, 14 cells). Significance for **D** was determined using a heteroscedastic Student's *t*-test; *p < 0.05, **p < 0.001.

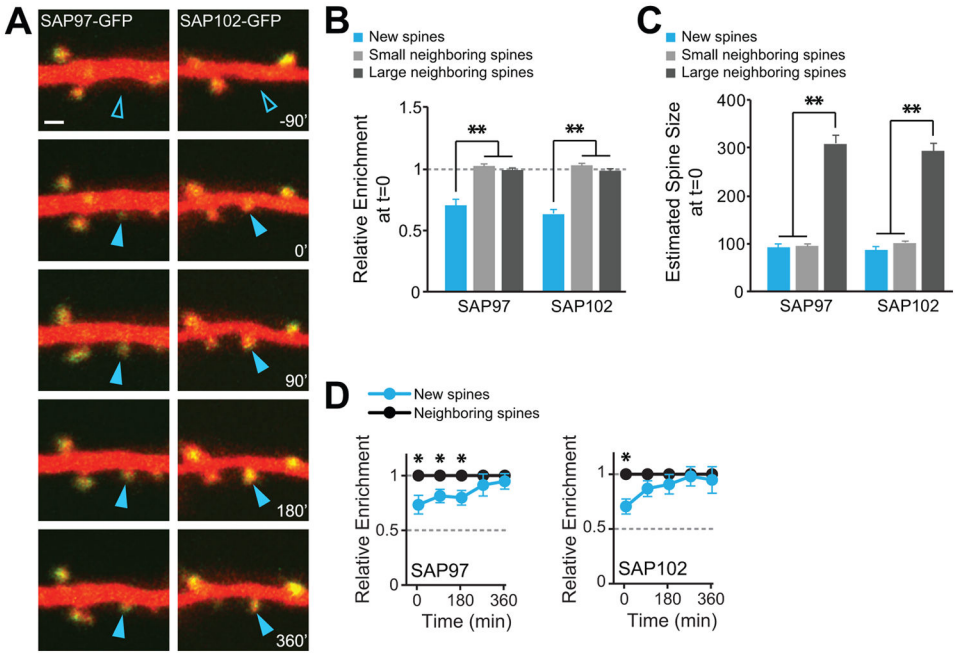

Figure 4. New spines have low levels of SAP97-GFP and SAP102-GFP, but accumulate mature levels of SAP102-GFP within 90 min and SAP97-GFP within 4.5 h

(A) Images of dendrites on CA1 neurons (DIV 7–12) expressing DsRed-Express and either SAP97-GFP (left panels) or SAP102-GFP (right panels). Blue arrowheads mark the sites of new spine growth before (open) and after (solid) initial appearance. Scale bar: 1 μm. **(B)** Relative enrichment of SAP97-GFP or SAP102-GFP in new spines is less than that of neighboring spines. SAP97-GFP: 136 new and 416 neighboring (187 small, 229 large) spines, 27 cells; SAP102-GFP: 97 new, 346 neighboring (144 small, 202 large) spines, 21 cells. **(C)** New spines are not different in size from small neighboring spines, but are smaller than large neighboring spines. **(D)** Relative enrichment of new spines (blue) is plotted over time relative to neighboring persistent spines (black) for SAP97-GFP (93 new and 291 neighboring spines, 20 cells) and SAP102-GFP (39 new and 151 neighboring spines, 12 cells). Significance for each time-point of **D** was determined using a heteroscedastic Student's *t*-test; *p < 0.05, **p < 0.001.

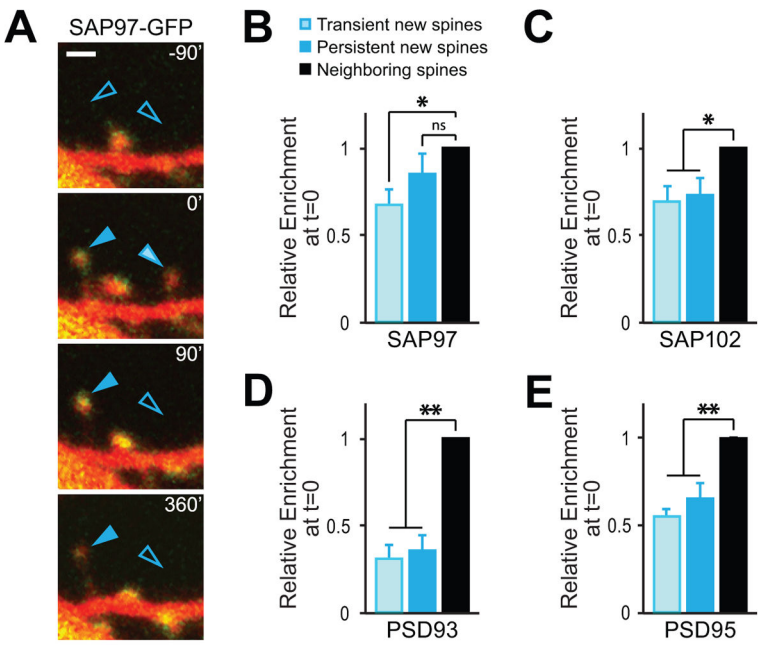

Figure 5. SAP97-GFP is at mature levels in persistent new spines when they first appear

(A) Time-lapse images of a dendrite expressing SAP97-GFP identifies two new spines, one with high levels of SAP97-GFP (blue), and one with low levels of SAP97-GFP (light blue), on the same dendritic segment. 90 min after initial appearance, the new spine with low levels of SAP97-GFP had disappeared, but the new spine with high levels of SAP97-GFP persisted until the end of the experiment at 360 min. Scale bar: 1 μm. **(B)** Relative enrichment of SAP97-GFP in new spines persisting to the end of the experiment (>360 min after spine identification, "persistent new spines", blue; 35 spines, 16 cells) was not different than that of persistent neighboring spines (black; 291 spines, 20 cells). However, new spines surviving <90 min ("transient new spines", light blue; 39 spines, 17 cells) had lower relative enrichment of SAP97-GFP than their persistent neighbors. **(C)** SAP102-GFP, **(D)** PSD93-GFP, and **(E)** PSD95-GFP were at lower levels in both transient and persistent new spines compared to their persistent neighbors. n = (spines, cells): SAP102: transient new (19, 10), persistent new (9, 8) neighboring (151, 12); PSD93: transient new (18, 11), persistent new (26, 10) and neighboring (164, 14); PSD95: transient new (19, 10), persistent new (7, 7), neighboring spines (158, 15). *$p < 0.05$, **$p < 0.001$.

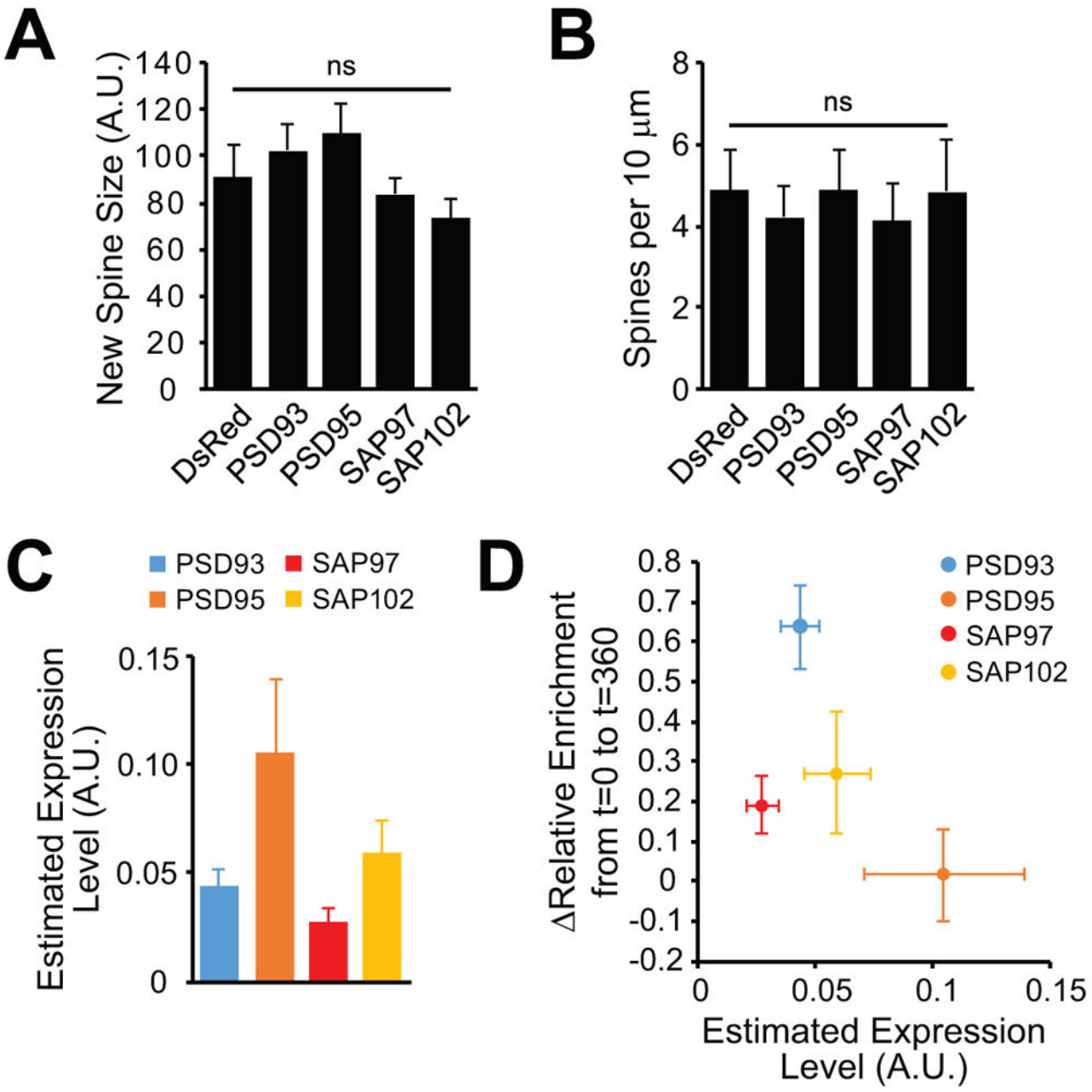

Figure 6. Arrival times of the PSD-MAGUKs at new spines are not correlated with expression levels

(A) New spines on cells expressing GFP-tagged PSD-MAGUKs and DsRed-Express were not different in size compared to those from cells expressing DsRed-Express alone. n = (new spines, cells): PSD93 (67, 14), PSD95 (45, 15), SAP97 (101, 20), SAP102 (51, 12). **(B)** Spine densities (from a randomly selected subset of the time-lapse data) were comparable between cells expressing GFP-tagged PSD-MAGUKs and DsRed-Express and those expressing DsRed-Express alone. n = (dendrites, cells): PSD93-GFP (13, 6), PSD95-GFP (8, 5), SAP97-GFP (11, 4), SAP102-GFP (14, 4), DsRed-Express (12, 5). **(C)** Estimated expression level of GFP-tagged PSD-MAGUKs. Expression level was estimated by

normalizing the green signal in persistent spines to the red signal of the dendritic shaft. n = (persistent spines, cells): PSD93-GFP (164, 14), PSD95 (158, 15), SAP97 (291, 20), SAP102 (151, 12). **(D)** There was no correlation between PSD-MAGUK expression level and change in the relative enrichment for PSD93-GFP, PSD95-GFP, SAP97-GFP, and SAP102-GFP in new spines from initial appearance (t = 0 min) to the final time point of the 6 h time-lapse (t = 360 min). Significance for **D** was determined using Pearson's correlation. *$p < 0.05$, **$p < 0.001$.

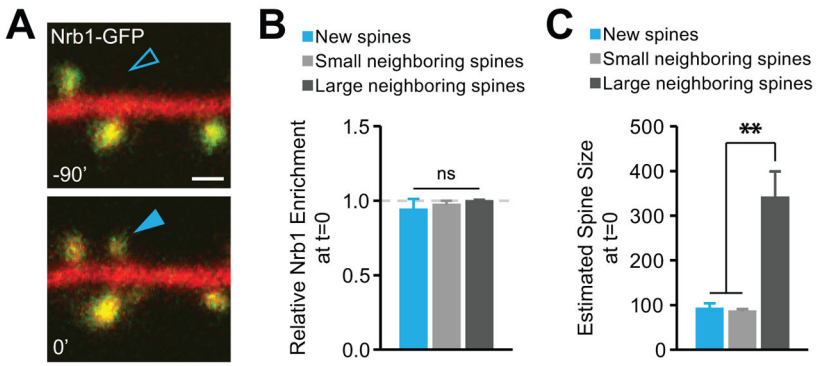

Figure 7. The actin-binding protein, Neurabin I, is at mature levels in new spines

(A) Images of a dendrite on a CA1 neuron (DIV 10) expressing Nrb1-GFP and DsRed-Express before and after a 90 min time-lapse revealing a new spine (blue arrowhead). Scale bar: 1 μm. **(B)** Relative enrichment for Nrb1-GFP is not different between new spines (blue) and either small (light gray) or large (dark gray) neighboring spines. **(C)** New spines are the same size as small neighboring spines, but are smaller than large neighboring spines. n = 24 new spines, 99 neighboring spines (34 small spines and 65 large spines), 8 cells. *p < 0.05, **p < 0.001.

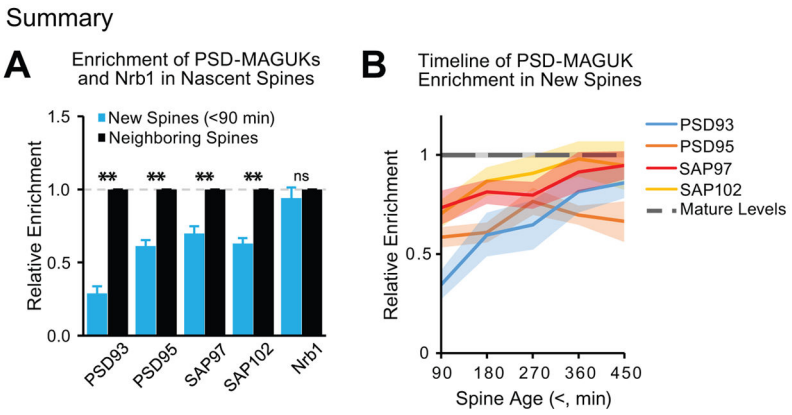

Figure 8. Summary Figure

(A) Relative enrichment of GFP-tagged PSD-MAGUKs or Nrb1 in new spines (<90 min old) compared to neighboring persistent spines. New spines are less enriched for PSD93-GFP, PSD95-GFP, SAP97-GFP, and SAP102-GFP, but not Nrb1-GFP. **(B)** Summary timeline of PSD-MAGUK enrichment in new spines. In general, new spines <90 min old are, on average, less enriched for all PSD-MAGUKs. New spines gained levels of SAP102-GFP comparable to persistent neighboring spines within 90 min of identification (<180 min old), and new spines gained mature levels of SAP97-GFP and PSD93-GFP within 270 min of identification (<360 min old). New spines that persisted to the end of the experiment (<450 min old) remained less enriched for PSD95-GFP. *p < 0.05, **p < 0.001.